Temperature dependence of solar cell performance—an analysis

Priyanka Singh*, N.M. Ravindra

Department of Physics, New Jersey Institute of Technology, Newark, NJ 07901, USA

ARTICLE INFO

ABSTRACT

This paper investigates, theoretically, the temperature dependence of the performance of solar cells in the temperature range 273–523 K. The solar cell performance is determined by its parameters, viz., short circuit current density (J_{sc}), open circuit voltage (V_{oc}), fill factor (FF) and efficiency (η). Solar cells based on semiconductor materials such as Ge, Si, GaAs, InP, CdTe and CdS are considered here. Reverse saturation current density (J_o) is an important diode parameter which controls the change in performance parameters with temperature. In this work, reverse saturation current density ($J_o = C.T^3.\exp(-qE_g/kT)$) is determined for three cases. Cases (I) and (II) correspond to $C = 17.90$ and 50 mA cm^{-2} K^3 respectively, whereas, case (III) corresponds to $C.T^3 = A = 1.5 \times 10^8$ mA cm^{-2}. The maximum achievable V_{oc}, J_{sc}, FF and η of solar cells are calculated for AM1.5G and AM0 spectra and are compared with theoretical and experimental results in the literature. Highest V_{oc}, FF and η are achieved for case (III). The performance of cells for case (III) gives the best agreement between the calculated and available theoretical and experimental data for solar cells based on the materials, Si, Ge, GaAs whereas, for InP, CdTe and CdS, case (I) seems to be more appropriate at 298 K. Moreover, as temperature changes, cases (I) and (II) are more suitable to describe the performance of solar cells. The rate of change of performance parameters with temperature, viz., dJ_{sc}/dT, dV_{oc}/dT, dFF/dT and $d\eta/dT$ are calculated and compared with the available data in the literature. In addition to theoretical results, the experimentally determined performance parameters of silicon solar cells and their rate of change with temperature are also presented.

© 2012 Elsevier B.V. All rights reserved.

1. Introduction

Solar cell is an optoelectronic device that can directly convert solar energy into electrical energy [1]. The study of the behavior of solar cells with temperature (T) is important as, in terrestrial applications, they are generally exposed to temperatures ranging from 15 °C (288 K) to 50 °C (323 K) [1] and to even higher temperatures in space and concentrator-systems [2]. Earlier studies [1–7] have pointed out that the performance of solar cells degrades with increase in temperature. The performance of a solar cell is determined by the parameters, viz., short circuit current density (J_{sc}), open circuit voltage (V_{oc}), fill factor (FF), and efficiency (η). The temperature variation affects these parameters and, hence, the performance of solar cells [1–8]. The diode parameters of solar cells, i.e., reverse saturation current density (J_o) and ideality factor (n) along with series resistance (R_s) and shunt resistance (R_{sh}) control the effect of temperature on V_{oc}, FF and η of the cell [5]. It has been shown earlier that V_{oc} decreases with increasing T whereas J_{sc} increases slightly with increasing T

[1–8]. Both FF and η decrease with increase in temperature and efficiency degradation is mainly due to decrease in V_{oc} [1–8]. The variation in R_s and R_{sh} with temperature affects slightly the efficiency [1–8], while exponential increase in J_o with increasing T decreases V_{oc} rapidly. Hence, J_o is a critical parameter affecting the efficiency of solar cells. J_o is a material dependent parameter and depends on the bandgap (E_g) of the material. Wysocki [1] and Fan [4] calculated the temperature dependence of the following solar cell parameters: E_g, V_{oc}, J_{sc}, FF and η of single junction solar cells ignoring the series and shunt resistances.

A single junction solar cell has maximum efficiency at an energy gap of around 1.35–1.5 eV [9]. In 1961, Shockley and Queisser showed that the maximum theoretical efficiency of a single solar cell is limited to 33% [10]. However, this limit could be overcome through the use of multiple cells, with varying band gaps, in a serial (tandem) arrangement [9,11]. Crystalline silicon (Si) has been the dominant material for photovoltaic (PV) cells for the past two decades. Nonetheless, other low cost semiconductor materials are better suited to absorb the solar energy spectrum [12] and are in development. Some are semiconductor thin-films such as amorphous silicon (a-Si), copper indium gallium diselenide (Cu(InGa)Se$_2$ or CIGS), and direct bandgap semiconductors from II–VI materials; for e.g., cadmium telluride (CdTe) and

* Corresponding author.
  E-mail address: priyankaph@gmail.com (P. Singh).

cadmium sulfide (CdS) are good candidates for use in solar cells [12]. Thin film CdTe solar cells are typically hetero-junctions with CdS being the n-type or window layer. Compound semiconductors from III–V materials such as gallium arsenide (GaAs), indium phosphide (InP) and gallium indium phosphide (GaInP) are used in concentrator technology and are more suitable for space applications [2,12]. Germanium (Ge) is generally used as the substrate and bottom cell in high-efficiency multijunction solar cells for applications in space. In a recent work, a stand-alone germanium solar cell process has been developed [13]. Besides, the temperature related studies will be important for further improvement in performance of these PV cells.

This paper investigates the temperature dependence of the performance parameters of solar cells based on the following semiconductor materials: Ge, Si, GaAs, InP, CdTe and CdS in the temperature range 273–523 K. The work presented in this paper will be useful in predicting the performance of single junction solar cells in the temperature range 273–523 K and can also be utilized further to study the temperature dependent performance of multi-junction, i.e., tandem solar cells. In this work, the maximum achievable open circuit voltage, short circuit current density, fill factor and efficiency of solar cells are predicted for AM1.5G and AM0 spectra, based on theory and experiment in the temperature range 273–523 K. The temperature dependence of reverse saturation current density, J_o and its effect on the parameters, V_{oc}, FF and η is discussed. Additionally, the experimentally obtained parameters J_{sc}, V_{oc}, FF and η of silicon solar cells are compared with calculated values.

2. Theoretical basis

Fig. 1 shows the equivalent circuit of an ideal solar cell. The current density–voltage (J–V) characteristics of p–n junction solar cells under steady state illumination can most simply be described using single exponential model as,

$$J = -J_{ph} + J_o(e^{qV/nKT} - 1) \qquad (1)$$

where, J_{ph} represents the photogenerated current density, V is the terminal voltage, i.e., voltage developed across the junction, k is the Boltzmann constant and n is the ideality factor. The variation in R_s and R_{sh} with temperature affects slightly the efficiency of a solar cell [1–8]. Therefore, in this work, R_s and R_{sh} are ignored. The diode ideality factor, n, is assumed to be 1 in this paper.

2.1. Data of solar spectra

The efficiency measurements of solar cells depend on the spectral distribution of the solar radiation and reference spectra that are needed for comparing their performance. Solar cell device parameter measurements are often reported with respect to an air mass 1.5 (AM1.5) standard or a reference spectra [14]. The American Society for Testing and Materials (ASTM) defines two standard terrestrial spectral distributions [14,15]; the direct-normal and global AM1.5. The direct normal irradiance standard at AM1.5 (AM1.5 D) represents the solar spectrum on earth, where the light is incident directly without any contribution from diffuse
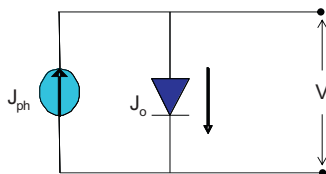
rays. However, Global AM1.5 (1000 Wm^{-2}, AM1.5G) represents the solar spectrum incident on the earth, and includes direct and diffuse rays from the sun. The AM1.5 G spectra are used as standards in the PV industry [14,15]. Calculations for situations in outer space can be performed with the solar spectral-irradiance spectra AM0 (1353 Wm^{-2}, AM0) [16]. For the purposes of calculations, all the data in this paper has been taken from Ref. [15].

2.2. General formulation

The equations discussed in the following section are well known in the literature. They are discussed here for completeness and for presenting the calculations. In this work, MATLAB version 2011b is used for all the calculations and modeling. In addition, Origin 8.5 is used for plotting and linear fitting of data.

When a solar cell is illuminated, only the photons having energy higher than the band gap energy (E_g) of the semiconductor are absorbed and create electron hole pairs [1]. The cut-off wavelength of photons of energy useful for carrier generation depends on E_g. The cut-off wavelength is given by,

$$\lambda_g = \frac{1240}{E_g(eV)} (nm) \qquad (2)$$

The photogeneration of electron–hole pairs in the semiconductor depends on the initial photon flux (N_{ph}) and the absorption coefficient (α_λ) of incident light in the semiconductor [1].

The temperature dependence of bandgap in semiconductors is described in literature [17–19]. Using Varshni relation temperature dependence of the bandgap in semiconductors can be described as

$$E_g(T) = E_g(0) - \frac{\alpha T^2}{(T + \beta)} \qquad (3)$$

where, E_g (T) is the band gap of the semiconductor at some temperature T, which may be direct or indirect, $E_g(0)$, its value at $T \approx 0$ K and α and β are constants. Table 1 lists the values of E_g (0), α and β for the semiconductor materials Si, Ge, GaAs, InP [17], CdTe and CdS [19].

The short circuit current density, J_{sc} depends on the given solar spectral irradiance and is given by,

$$J_{sc} = q \int_{hv = E_g}^{\infty} \frac{dN_{ph}}{dhv} d(hv) \qquad (4)$$

In a practical solar cell, the value of J_{sc} may be limited by reflection losses, ohmic losses (series and shunt resistance), shadowing losses (front metal coverage) and recombination losses. The values of J_{sc} are calculated using Eq. (4) at various temperatures. To calculate J_{sc} at each temperature, the solar spectrum is integrated to the corresponding value of E_g given by Eq. (3). The rate of change in J_{sc} with T, dJ_{sc}/dT is then calculated by linear fitting of data.

Fig. 1. Equivalent circuit of an ideal solar cell.

Table 1
Energy gap parameters for the semiconductor materials Si, Ge, GaAs, InP [17], CdTe and CdS [19].

Material	$E_g(0)$ (eV)	α (eV K^{-1}) $\times 10^{-4}$	β(K)
Si [17]	1.1557	7.021	1108
Ge [17]	0.7412	4.561	210
GaAs [17]	1.5216	8.871	572
InP[17]	1.4206	4.906	93
CdTe [19]	1.6077	3.100	108
CdS [19]	2.583	4.020	147

The open-circuit voltage is the maximum voltage available from a solar cell. Eq. (1) at $J=0$ yields the expression for V_{oc} as:

$$V_{oc} = \frac{kT}{q}\ln\left(\frac{J_{sc}}{J_0}+1\right) \tag{5}$$

where, $J_{sc} \approx J_{ph}$, V_{oc} is related to J_{sc} and J_o and hence to E_g. For a high V_{oc}, a low J_o is absolutely necessary.

The temperature dependence of V_{oc} can be obtained from Eq. (5) as

$$\frac{dV_{oc}}{dT} = \left(\frac{V_{oc}}{T}\right) + V_{th}\left(\frac{1}{J_{sc}}\frac{dJ_{sc}}{dT}-\frac{1}{J_o}\frac{dJ_o}{dT}\right) \tag{6}$$

where, $V_{th}=kT/q$.

Reverse saturation current density, J_o, is a measure of the leakage (or recombination) of minority carriers across the p–n junction in reverse bias. This leakage is a result of carrier recombination in the neutral regions on either side of the junction and, therefore J_o, primarily controls the value of V_{oc} in the solar cells. The minority carriers are thermally generated; therefore, J_o is highly sensitive to temperature changes. Reverse saturation current density, J_o, for a p–n junction solar cell, has been modeled [20] as:

$$J_o = q\left(\frac{D_n}{L_n N_A}+\frac{D_p}{L_p N_D}\right)n_i^2 \tag{7}$$

where, n_i is the intrinsic carrier density, N_A and N_D are densities of acceptor and donor atoms, D_n and D_p are diffusion constants of minority carriers in p and n regions, L_n and L_p are diffusion lengths of minority carriers in n and p regions, respectively. As from Eq. (7), J_o is strongly determined by the proportionality to $\sim n_i^2$ and n_i can be represented as:

$$n_i^2 = N_c N_v \exp\left(-\frac{E_g}{kT}\right) = 4.\left(\frac{2\pi kT}{h^2}\right)^3 m_e^{*3/2}m_h^{*3/2}\exp\left(-\frac{E_g}{kT}\right) \tag{8}$$

where, N_c, N_v are effective density of states in conduction band, valance band and m_e, m_h are effective mass of electron, hole respectively.

Combining Eqs. (7) and (8), the expression for J_o can be written in terms of temperature and bandgap energy [21] as:

$$J_0 = C.T^3.\exp\left(-\frac{E_g}{k.T}\right) \tag{9a}$$

In the above equation, doping and the material parameters of solar cells are combined in this one constant C [21]. The important solar cell parameters for the model calculations are the temperature and bandgap. The higher the bandgap, lower will be the saturation current density.

Green has proposed a simple empirical relation [22] for J_o where the product $C.T^3$ is replaced by a constant $A=1.5\times10^8$ mA cm^{-2} [22]:

$$J_0 = A.\exp\left(-\frac{qE_g}{k.T}\right) \tag{9b}$$

Taking natural logarithm on both sides of Eqs. (9a) and (9b) and, then, differentiating with respect to T, we have the following expressions respectively:

$$\frac{1}{J_o}\frac{dJ_o}{dT} = \frac{3}{T}-\frac{1}{V_{th}}\left(-\frac{E_g}{T}+\frac{dE_g}{dT}\right) \tag{10a}$$

$$\frac{1}{J_o}\frac{dJ_o}{dT} = -\frac{1}{V_{th}}\left(-\frac{E_g}{T}+\frac{dE_g}{dT}\right) \tag{10b}$$

The Eq. (10a) and (10b) are used to determine the temperature coefficient $(1/J_o)(dJ_o/dT)$.

A combination of Eqs. (3) and (6) with (10a) and (10b) give the following expressions for dV_{oc}/dT as:

$$\frac{dV_{oc}}{dT} = \left(\frac{V_{oc}}{T}\right) + V_{th}\frac{1}{J_{sc}}\frac{dJ_{sc}}{dT}-\left(\frac{3V_{th}}{T}+\frac{E_g(0)}{T}+\frac{\alpha T}{(T+\beta)^2}\right) \tag{11a}$$

$$\frac{dV_{oc}}{dT} = \left(\frac{V_{oc}}{T}\right) + V_{th}\frac{1}{J_{sc}}\frac{dJ_{sc}}{dT}-\left(\frac{E_g(0)}{T}+\frac{\alpha T}{(T+\beta)^2}\right) \tag{11b}$$

Eqs. (11a) and (11b) are used to calculate the dV_{oc}/dT values in the temperature range 273–523 K.

Fill factor is defined as the ratio of the maximum power output (P_{max}) at the maximum power point to the product of the open-circuit voltage and short-circuit current density and can be expressed as:

$$FF = \frac{P_{max}}{V_{oc}J_{sc}} \tag{12}$$

Green [22] gave an expression for the calculation of FF to an excellent accuracy,

$$FF = \frac{v_{oc}-\ln(v_{oc}+0.72)}{v_{oc}+1} \tag{13}$$

where, $v_{oc} = (V_{oc}/V_{th})$ is defined as 'normalized V_{oc}'.

Eq. (12) is more suitable for calculating FF of an experimental I–V curve of a solar cell as well as it considers the effect of R_s and R_{sh} on the performance of the cell. However, this work is intended to calculate the theoretical FF in ideal cases and Eq. (13) gives maximum possible value of FF, and it does not consider resistive losses [22]. Therefore, in this paper, Eq. (13) has been used to calculate FF. Fill factor is calculated at each temperature using Eq. (13) corresponding to the calculated V_{oc} at each temperature. The temperature dependence of FF with T can be determined from Eq. (13) as:

$$\frac{dFF}{dT} = \frac{(dV_{oc}/dT-V_{oc}/T)}{(V_{oc}+V_{th})}\left\{\frac{(V_{oc}/V_{th}-0.28)}{(V_{oc}/V_{th}+0.72)}-FF\right\} \tag{14}$$

The rate of change of FF with T, i.e., dFF/dT, is determined by combining Eqs. (14), (11a) and (11b).

The efficiency of a solar cell is the ratio of the power output corresponding to the maximum power point to the power input and is represented as:

$$\eta = \frac{P_{max}}{P_{in}.Area} \quad or \quad \eta = \frac{V_{OC}.J_{SC}.FF.}{P_{in}} \tag{15}$$

where, P_{in} is the intensity of the incident radiation.

Efficiency is calculated at each temperature using Eq. (15) corresponding to the calculated V_{oc}, J_{sc} and FF at each temperature. $d\eta/dT$ is then estimated by fitting the data in Origin.

3. Results and discussion

The temperature dependence of J_o is determined using Eqs. (10a) and (10b). Loferski has discussed the cases where $C.T^3$ is equal to 1×10^8 mA cm^{-2} and 1.44×10^8 mA cm^{-2} [23]. The Eq. (10a) is based on a fit to experimentally achieved open-circuit voltages [21]. An optimized value of $C=17.90$ mA cm^{-2} K^3 has been used by Nell [21] for the calculation of performance parameters of solar cells made from a variety of materials [21]. Therefore, for an optimized solar cell design, a minimum value of C is required and in reality a single value is not applicable to all materials. Fan chose a value of $C=50$ mA cm^{-2} K^3 [24]. Nell investigated the effect of various values of C on the performance parameters of solar cells and found that the constant C affects the efficiency logarithmically and a reasonable variation in the value of C, around 17.90 mA cm^{-2} K^3, will only have a modest effect on

the overall system efficiency [21]. However, to investigate the effect of J_o on performance parameters, in this work, three cases are considered for the calculation of J_o: (I) $C=17.90$ mA cm^{-2} K^3 (Eq. (9a)) [21], (II) $C=50.0$ mA cm^{-2} K^3 (Eq. (9a)) [24] and (III) $A=C.T^3=1.5\times10^8$ mA cm^{-2} (Eq. (9b)) [22]. In the following section, J_o and its effect on the performance parameters, V_{oc}, FF and efficiency, for these three cases is discussed in the temperature range 273–523 K.

For solar cells based on each material, Eq. (9a) is modeled for cases (I) and (II) and Eq. (9b) is used for case (III). The obtained values of J_o are plotted in Fig. 2a. Fig. 2a shows an Arrhenius plot of J_o for Si for the three cases described above in the temperature range 273–523 K. This figure shows the temperature dependence of J_o and summarizes the effect of the parameters A and C on J_o values. As expected, J_o is noticeably different for the three cases. J_o values for case (I) ($C=17.90$) and case (II) ($C=50$) are close to each other whereas, for case (III) ($A=1.5\times10^8$), J_o differs significantly. Lowest J_o values are obtained for $A=1.5\times10^8$. It is worthwhile to note here that J_o corresponds to recombination in neutral regions; higher J_o corresponds to more leakage or recombination of carriers

whereas lower J_o corresponds to less recombination. The temperature coefficient $(1/J_o)$ (dJ_o/dT) is determined using Eq. (10a) and (10b). The $(1/J_o)$ (dJ_o/dT) values are noted in Fig. 2a along with J_o values at 298 K for the three cases. It can be seen that $(1/J_o)(dJ_o/dT)$ is lower for case (III) as compared to case (I) and case (II). The temperature coefficient, $(1/J_o)$ (dJ_o/dT) decreases with increasing temperature in each case. Similar observation is also seen for solar cells based on GaAs, Ge, InP, CdTe and CdS (due to similarity in their general behavior, Arrhenius plots are not shown). The calculated J_o values for the three cases are used to compute the parameters, V_{oc}, FF and efficiency. The calculated performance parameters are then compared with the theoretical and experimental data available in the literature. It will be discussed later (Table 2) that the modeling results for case (III) $A=1.5\times10^8$ mA cm^{-2} gives the best agreement between the calculated and available experimental and theoretical data for solar cells based on Si, Ge and GaAs whereas, for solar cells based on InP, CdTe and CdS, case (I) $C=17.90$ seems to be more appropriate at 298 K. Fig. 2b shows Arrhenius plots of J_o for solar cells based on Ge, Si, InP, GaAs, CdTe and CdS. It can be seen from Fig. 2a and b that J_o
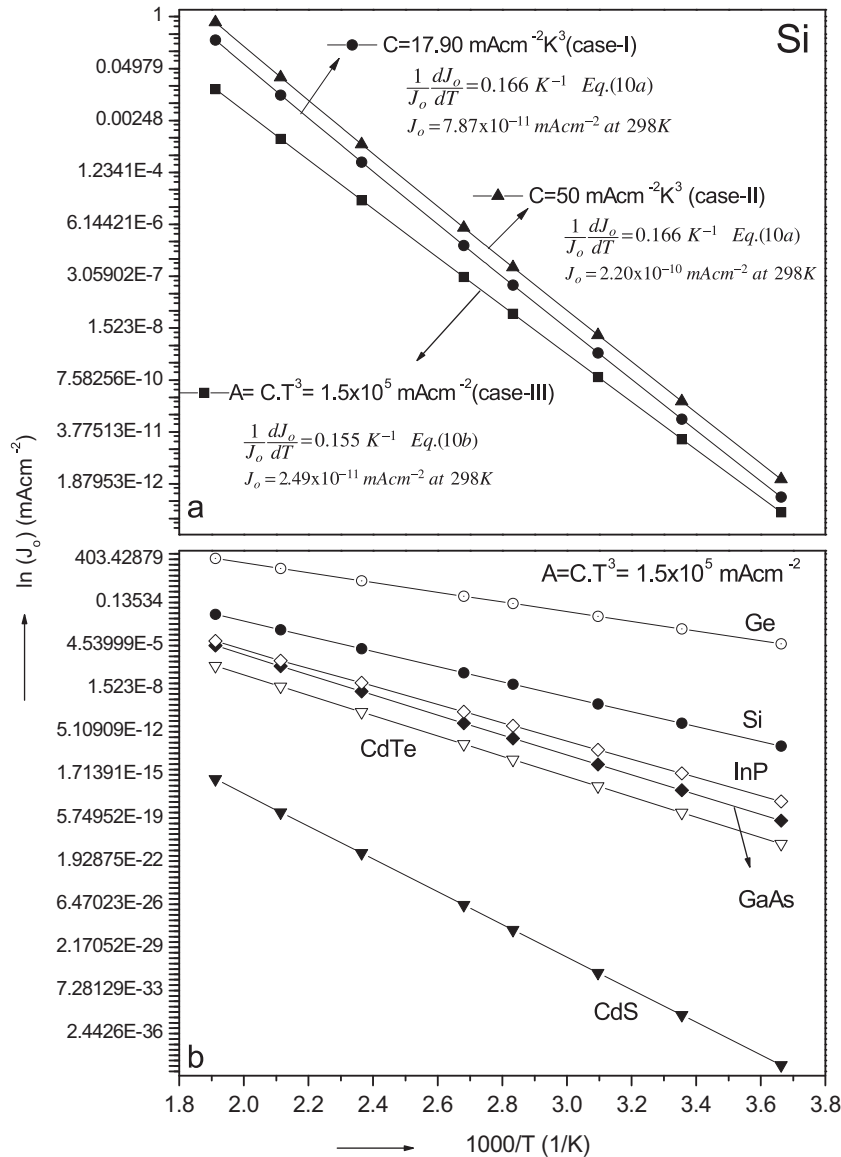
Fig. 2. Arrhenius plots of J_o in the temperature range 273–523 K: (a) for Si solar cells for three cases: (I) $C=17.90$ mA cm^{-2} K^3 (Eq. (9a)) [21], (II) $C=50.0$ mA cm^{-2} K^3 (Eq. (9a)) [24] and (III) $A=C.T^3=1.5\times10^8$ mA cm^{-2} (Eq. (9b)) [22]. (b) for solar cells based on Ge, Si, InP, GaAs, CdTe and CdS for case (III).

Table 2

Theoretically and experimentally achieved maximum J_{sc}, V_{oc}, FF and efficiency reported by several authors [2–4,12,28,30] including present work for solar cells based on Si, Ge, GaAS, InP, CdTe and CdS at room temperature 298 K for spectra AM1.5G and AM0.

		J_{sc} (mA cm^{-2})	V_{oc} (V)	FF	η (%)	J_{sc} (mA cm^{-2})	V_{oc} (V)	FF	η (%)
		Si				**Ge**			
I[a]	AM 1.5G	44.11	0.695	0.846	25.94	61.03	0.254	0.691	10.70
	AM 0	53.61	0.700	0.847	23.49	81.19	0.261	0.696	10.91
II[a]	AM 1.5G	44.11	0.669	0.842	24.83	61.03	0.227	0.669	9.28
	AM 0	53.61	0.674	0.842	22.49	81.19	0.235	0.675	9.51
III[a]	AM 1.5G	44.11	0.725	0.851	27.19	61.03	0.283	0.712	12.31
	AM 0	53.61	0.729	0.851	24.62	81.19	0.291	0.717	12.50
[28]	AM1.5G [b]	42.7	0.706	0.83	25.0 ± 0.5	46.40[12]	0.269[12]	0.624[12]	7.8 [12]
[2][c]	AM0				∼23.0				∼13.85
[3][c]					∼22.04				∼13.02
[4][c]	AM1	38.60	0.699	0.85	24.67	57.64	0.248	0.69	10.60
		GaAs				**InP**			
I[a]	AM 1.5G	31.61	1.006	0.883	28.10	34.67	0.929	0.876	28.19
	AM 0	38.61	1.011	0.884	25.51	42.10	0.934	0.876	25.46
II[a]	AM 1.5G	31.61	0.980	0.881	27.29	34.67	0.902	0.873	27.31
	AM 0	38.61	0.985	0.881	24.78	42.10	0.907	0.874	24.66
III[a]	AM 1.5G	31.61	1.036	0.886	29.01	34.67	0.958	0.879	29.19
	AM 0	38.61	1.041	0.886	26.33	42.10	0.963	0.879	26.35
[28]	AM1.5G [b]	29.6	1.107	0.84	27.6 ± 0.8	29.5	0.878	0.85	22.1 ± 0.7
[2][c]	AM0				∼23.62				∼23.60
[3][c]					∼26.90				∼25.53
[4][c]	AM1	29.40	0.989	0.88	27.73				
		CdTe				**CdS**			
I[a]	AM 1.5G	28.2	1.111	0.892	27.93	7.49	2.041	0.933	14.26
	AM 0	34.40	1.116	0.892	25.31	9.39	2.047	0.933	13.26
II[a]	AM 1.5G	28.2	1.111	0.892	27.93	7.49	2.041	0.933	14.26
	AM 0	34.40	1.116	0.892	25.31	9.39	2.047	0.933	13.26
III[a]	AM 1.5G	28.2	1.140	0.894	28.74	7.49	2.071	0.934	14.48
	AM 0	34.40	1.145	0.894	26.04	9.39	2.076	0.934	13.46
[28]	AM1.5G [b]	26.1	0.845	0.76	16.7 ± 0.5 17.3				
[30]					17.3				
[2][c]	AM0				∼23.62				∼12.83
[3][c]					∼27.37				∼13.06

[a] Calculations done in this work. I, II and III correspond to three cases of J_o calculations: (I) $C = 17.90$ mA cm^{-2} K^3 (Eq. (9a)), (II) $C = 50.0$ mA cm^{-2} K^3 (Eq. (9a)) and (III) $A = C.T^3 = 1.5 \times 10^8$ mA cm^{-2} (Eq. (9b)).

[b] Experimentally reported performance parameters.

[c] Theoretically reported performance parameters.

increases with increasing temperature whereas it decreases with increasing bandgap. It can also be seen from Fig. 2a that Ge has very high J_o values which can be attributed to the low bandgap of Ge [25]. Consequently, it decreases the V_{oc} and efficiency especially at temperatures higher than 400 K (Fig. 4).
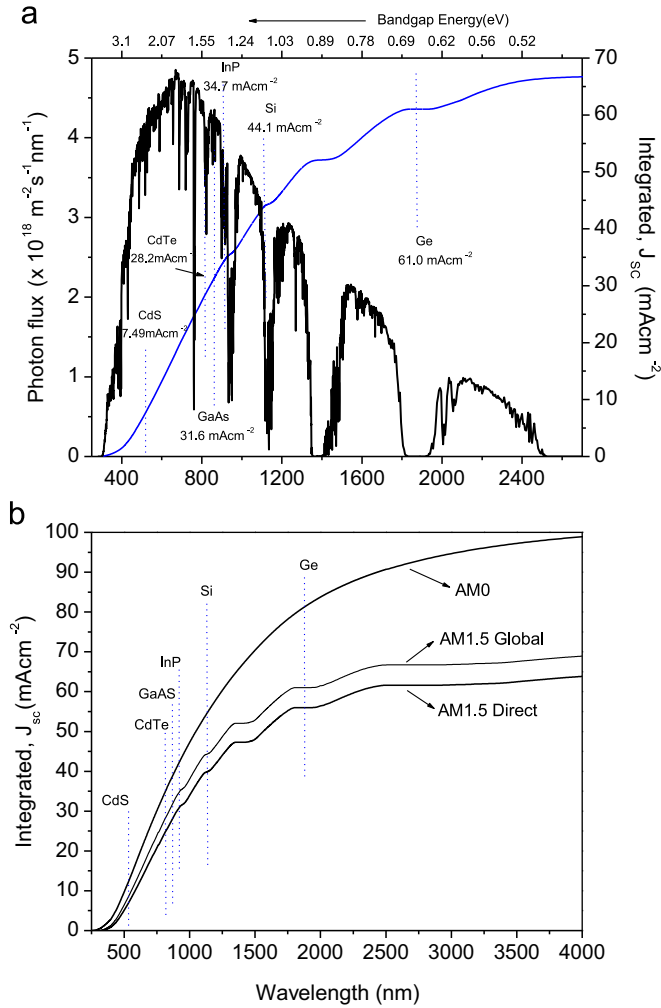
The maximum achievable short circuit current density, J_{sc}, dependent on the bandgap, is calculated directly from spectral data. The units of spectral data are typically given as spectral irradiance (Wm^{-2} nm^{-1}), which can be easily converted to N_{ph} (m^{-2} s^{-1} nm^{-1}). Eq. (4) can be used to calculate the maximum attainable J_{sc} for a solar cell, which is the integral of the AM1.5 (or AM0) photon flux curve up to the bandgap of the absorber materials (Fig. 3a) and Refs. [26,27]). The variation in photon flux and J_{sc} with wavelength (or bandgap-top x axis) is illustrated in Fig. 3a. The maximum obtainable J_{sc} for solar cells based on materials Ge, Si, InP, GaAs, CdTe and CdS are denoted by dotted lines in Fig. 3a. The maximum J_{sc} at temperature 298 K for solar cells based on these materials in mA cm^{-2} are: Ge-61.0, Si-44.1, InP-34.7, GaAs-31.6, CdTe-28.2 and CdS-7.49. Similarly, the current density is integrated for AM1.5D and AM0 spectra. Fig. 3b shows the variation in maximum achievable J_{sc} for AM0, AM1.5 D and AM 1.5G spectra with wavelength. The maximum achievable J_{sc}, as a function of bandgap, calculated for AM1.5G and AM1.5D in this work are same as reported in a recent work [27]. Current density is higher for AM0 spectra as compared to AM1.5 G and AM1.5D. For example, the maximum J_{sc} for silicon solar cells in mA cm^{-2} under spectra AM0, AM1.5G and AM1.5D are 54.67, 44

and 39.86 respectively. Thus far, for silicon solar cells, the measured J_{sc} in laboratory cells is ∼42 mA cm^{-2} while in commercial solar cells, it is in the range ∼28–35 mA cm^{-2} [28]. Table 2 lists the J_{sc} values calculated at a temperature of 298 K for all the materials for AM1.5G and AM0 spectra.

The changes in performance parameters, J_{sc}, V_{oc}, FF and η with temperature for solar cells based on Ge, Si, InP, GaAs, CdTe and CdS in the temperature range 273–523 K are reported in Fig. 4. Experimentally achieved J_{sc}, V_{oc}, FF and efficiency measured under AM1.5G spectrum at 298 K for solar cells based on all the available photovoltaic materials have been reported by Green et al. [28]. The theoretically achieved maximum J_{sc}, V_{oc}, FF and efficiency for solar cells based on these materials are reported by Wysocki and Rappaport [2] (under AM0 spectrum) and Fan [4] (under AM1 spectrum) with varying temperature. Table 2 lists the theoretically and experimentally achieved maximum J_{sc}, V_{oc}, FF and efficiency reported by several authors [1,2–4,28] including the present work for solar cells based on Si, Ge, GaAs, InP, CdTe and CdS at room temperature of 298 K. In Table 2, V_{oc}, FF and efficiency are calculated for the three cases described above. These parameters are calculated for AM1.5 G and AM0 spectra. Table 2 also describes the effect of J_o on the solar cell performance parameters.

The variation in J_{sc} with temperature for solar cells based on Ge, Si, InP, GaAs, CdTe and CdS is presented in Fig. 4a. As can be seen in the figure, J_{sc} increases with increasing temperature whereas it decreases with increasing bandgap. It can be seen

Fig. 3. (a) Photon flux from the sun at the earth's surface ($1000 \, \mathrm{Wm^{-2}}$, AM1.5G) and the integrated short circuit current density as a function of wavelength (bandgap—top x axis). The integrated J_{sc} is shown on the right y-axis. (b) variation in maximum achievable J_{sc} for AM0, AM1.5 D and AM 1.5G spectra with wavelength.

from Table 2 that, for solar cells based on Si, GaAs, InP and CdTe, the maximum J_{sc} calculated in this work is very close to the values reported by other authors [1,2,4,27] as well as to the reported experimental values [28]. However, for Ge based cells, the difference in experimental [12] and theoretical values is high. Variation in short circuit current density with temperature is primarily due to the change in bandgap with temperature [1]. Generally, for most semiconductors, as the temperature increases, the bandgap decreases [1]. Consequently, the solar cell responds to longer wavelength regions in the solar spectrum and J_{sc} increases. Thus, J_{sc} is roughly proportional to the incident spectral intensity at wavelengths near the band edge [29].

The variation in the open circuit voltage for solar cells based on Ge, Si, InP, GaAs, CdTe and CdS in the temperature range 273–523 K is shown in Fig. 4b. Open-circuit voltages shown in Fig. 4b are determined from the calculated J_{sc} and J_o using Eq. (5) for case (III) only. Table 2 lists the values of V_{oc} calculated for three cases at 298 K described above. Additionally, in Table 2, V_{oc} values are calculated for both AM1.5G and AM0 spectra. It has been observed earlier that the open-circuit voltage shows an insignificant dependence on AM0, AM1, AM1.5G and AM.1.5D spectra [21]. According to Eq. (5), the voltage will increase if the light intensity is increased. However, only a small difference in V_{oc} is observed if spectrum AM0 or AM1.5 is used [21]. In this

work, the calculated V_{oc} for spectra AM1.5G and AM0 are almost the same (Table 2). It can also be observed from Table 2 that V_{oc} depends on J_o (for three cases) critically, and hence, on E_g (Eq. (5)) [1]. The maximum V_{oc} values are obtained for case (III) whereas lowest values are obtained for case (I). For solar cells based on Si, Ge and GaAs, the V_{oc} calculated for case (III) are very close to the experimentally achieved V_{oc}. However, for solar cells based on InP and CdTe, the V_{oc} calculated for case (I) are more close to the experimentally achieved V_{oc}. CdS is generally used as an n-type or absorber layer in CdTe solar cells. Therefore, no experimental V_{oc} is reported. Nonetheless, the values calculated in this work are close to the values reported by Wysocki and Rappaport [2]. It can be seen from Fig. 4b that V_{oc} decreases with increasing temperature whereas it increases with increasing bandgap. For solar cells based on Ge, at 373 K, V_{oc} value is 0.159 V and decreases further to 0.006 V at 523 K. The decrease in bandgap with increasing temperature results in lower V_{oc}. It is important to note here that $V_{oc} \leq 0.1$ V are reported for temperature higher than 373 K by Fan [4] for AM1 spectra and by Wysocki and Rappaport [2] for AM0 spectra. The slight difference in both reported [2,4] and calculated V_{oc} in this work may be attributed to different spectra as well as to the J_o values. It can be seen from Table 2 that, for solar cells made from almost all the materials, the maximum achievable V_{oc} calculated in this work is quite close to the values reported by other authors [1,2–4,27] as well as to the reported experimental values [28].

Fig. 4c shows the change in fill factor with temperature for solar cells based on Ge, Si, InP, GaAs, CdTe and CdS in the temperature range 273–523 K. Fill factor is determined with the Green's formula [22] (Eq. (13)) from the calculated V_{oc}. It can be seen from Fig. 4c that FF decreases with increasing temperature. It is important to mention here that Eq. (13) gives approximately the ideal FF and is only dependent on V_{oc}. Nonetheless, it can be seen from Table 2 that the calculated FF values in this work are very close to the reported theoretical values [2,4] as well as to the experimental values [27] for solar cells based on almost all the materials. The decrease in FF is mainly controlled by decrease in V_{oc} whereas increase in J_{sc} with temperature does not contribute much to FF [5].

Fig. 4d–f shows the variation of efficiency for solar cells based on Ge, Si, InP, GaAs, CdTe and CdS in the temperature range 273–523 K for the three cases described above. The maximum achievable efficiency for each solar cell is computed using Eq. (15) based on the calculated current density, open circuit voltage and fill factor. Fig. 4d–f shows the change in efficiency with T for solar cells based on Si, Ge, GaAs, InP, CdTe and CdS solar cells respectively. In Fig. 4d–f, the solid ($\bullet$) and '+' symbols represent case (I) and (II) whereas open ($\circ$) symbol represents the case (III). As can be seen from the figures, the efficiency decreases with temperature. The higher efficiencies are obtained for case (III) whereas lower efficiencies are obtained for case (II). It can be seen from Fig. 4d–f that almost all the materials show similar behavior for these three cases. It can be seen among all the materials that Ge has lowest efficiency whereas InP and GaAs show highest efficiencies. For Ge, at 373 K, efficiencies for cases (I) and (II) are 2.70% and 1.53% while for case (III), efficiency is 5.26%. It is important to mention here that for Ge, $\eta = 2.79\%$ is reported by Fan [4] at 373 K. The efficiency decreases further with increasing temperature. This decrease in efficiency with T for Ge is expected as V_{oc} decreases to low values as shown in Fig.4b. Table 2 lists the efficiencies calculated for spectra AM1.5G and AM0 for each material at 298 K. Efficiencies calculated for solar cells based on Si, Ge and GaAs for case (III) are very close to the experimentally achieved efficiencies. However, for solar cells based on InP and CdTe, the η calculated for case (I) is more close to the experimentally achieved efficiencies. Nevertheless, the experimentally
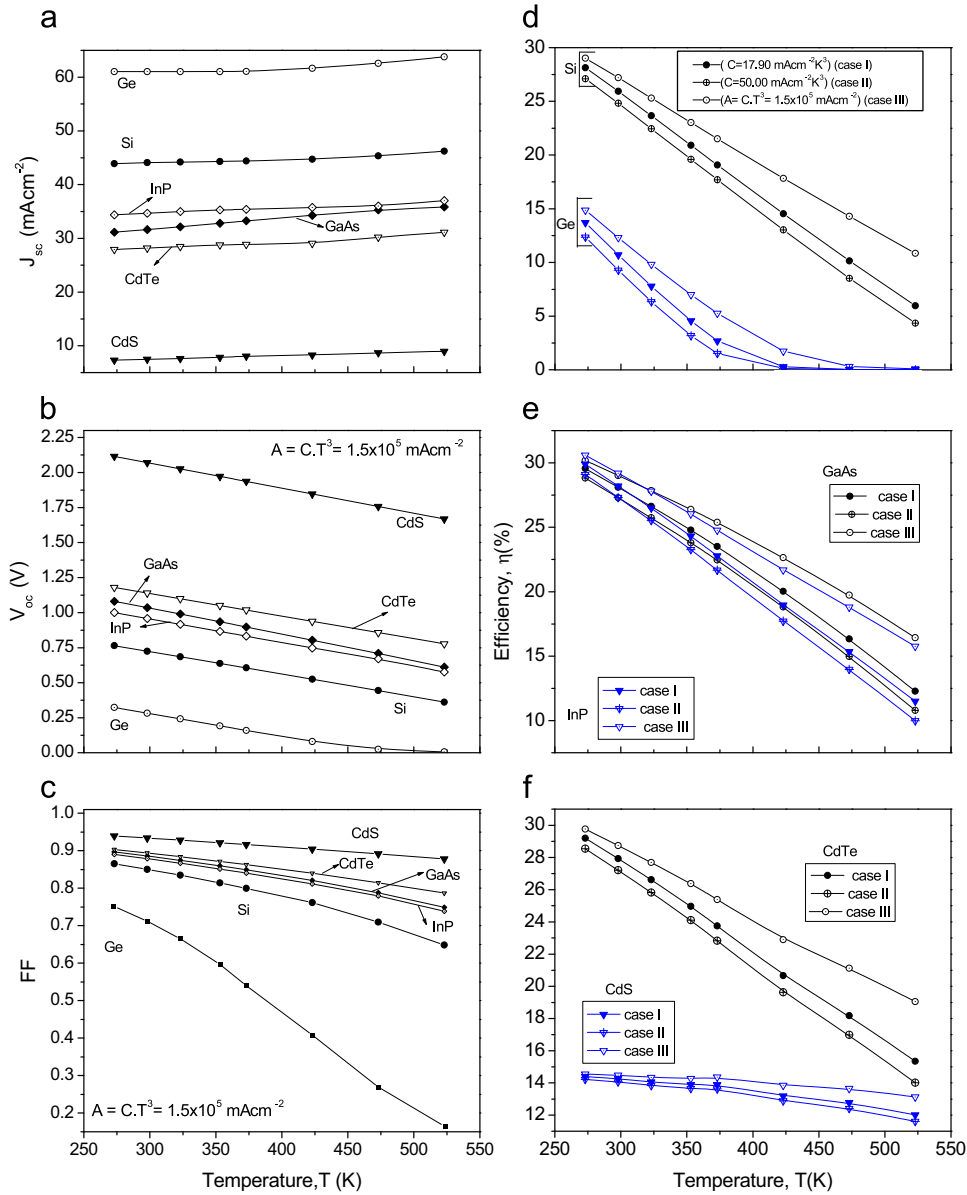
Fig. 4. Variations in solar cell performance parameters; (a) J_{sc}. (b) V_{oc}. (c) FF. (d) η for Ge, Si (e) η for GaAs, CdTe and (f) η for CdTe and CdS with temperature for solar cells in the temperature range 273 K–523 K. In (b) and (c) V_{oc} and FF are computed for case (III). In (d–f), η is calculated for three cases (I), (II) and (III), the solid (●) and '+' symbols represent cases (I) and (II) whereas open (○) symbol represents the case (III).

achieved efficiencies are lower than ideal due to several reasons such as resistive and reflective losses. The difference in experimental and theoretical efficiencies for Si and GaAs are $\sim 8 \pm 2\%$ and $\sim 5 \pm 3\%$ respectively. However, for solar cells based on Ge, InP and CdTe, this difference is larger; $\sim 36\%$, $\sim 22 \pm 2\%$ and $\sim 40 \pm 2\%$ respectively. In thin film CdTe/CdS solar cells, continuous efforts are in progress to reduce this difference.

The rate of change in J_{sc}, V_{oc}, FF and efficiency with temperature, i.e. dJ_{sc}/dT, dV_{oc}/dT, dFF/dT and $d\eta/dT$, are calculated by linear fitting the data (Fig. 4). These values are listed in Table 3 for cases (I), (II) and (III). The obtained values of dJ_{sc}/dT are slightly different for cells based on each material. However, for solar cells based on Si, Ge and GaAs, dJ_{sc}/dT matches fairly well with values reported by Fan [4]. The dV_{oc}/dT values are also calculated from Eqs. (11a) and (11b) and are plotted for Si in Fig. 5a in the temperature range 273–523 K along with the values obtained by Fan [4]. In Eq. (11a), the extra term, $-3V_{th}/T$, corresponds to cases (I) and (II) as compared to Eq. (11b) which corresponds to case (III). Consequently, the rate of decrease of V_{oc} with T i.e., dV_{oc}/dT is

higher for cases (I) and (II) as compared to case (III). This can be observed from Fig. 5a and that, for all the solar cells based on the materials considered in this study, dV_{oc}/dT decreases more rapidly with T for case (II) as compared to case (I) and (III). The decrease in V_{oc} is mainly controlled by the decrease in E_g with increasing temperature. The rate of decrease in FF with T, i.e., dFF/dT is determined from Eq. (14) and is plotted for Si in Fig. 5b in the temperature range of 273–523 K along with the values obtained by Fan [4]. It can be seen from Fig. 5b that the rate of decrease of FF with temperature is slower for case (III) as compared to case (I) and (II). In addition, FF decreases at higher rate as temperature increases (Fig. 5b). Similarly η decreases at higher rate for case (II) as compared to cases (I) and (III). It can be seen from Table 3 that dFF/dT and $d\eta/dT$ are different for each solar cell candidate material whereas dV_{oc}/dT is more or less same for each material. Nevertheless, dV_{oc}/dT, dFF/dT and $d\eta/dT$, calculated in this work, represent the values for ideal or high quality solar cells (as R_s, R_{sh} and their temperature dependence are ignored and n is considered to be equal to 1 in this work). Therefore, the rate of decrease

Table 3
Rate of change of performance parameters with temperature: dJ_{sc}/dT, dV_{oc}/dT, dFF/dT and $d\eta/dT$ for solar cells based on Ge, Si, InP, GaAs, CdTe and CdS for cases (I), (II) and (III).
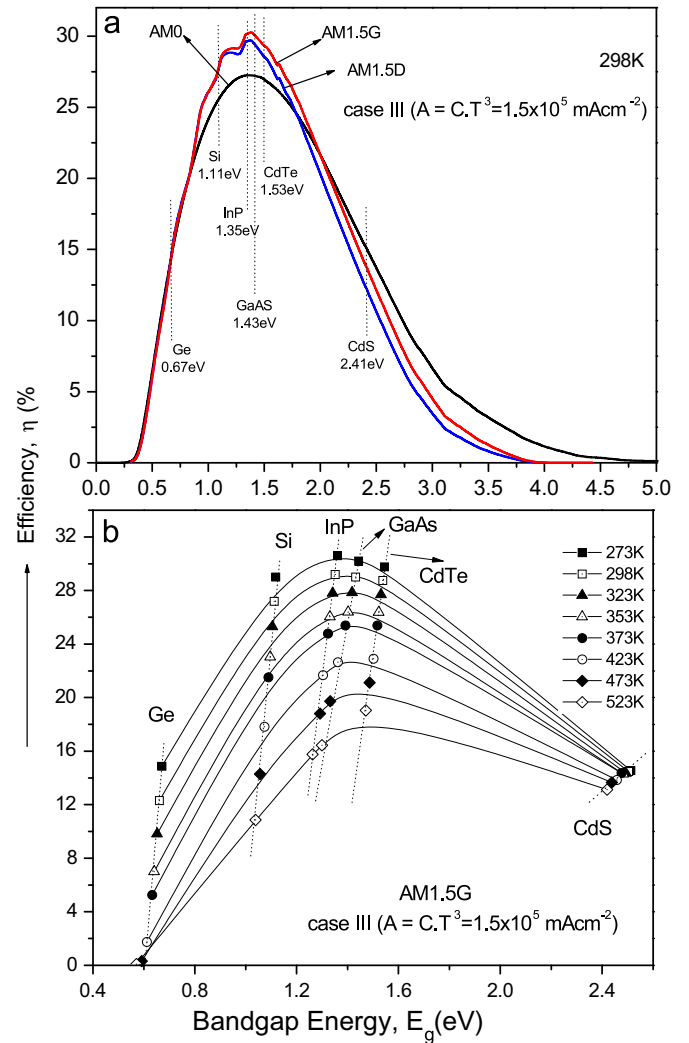
	dJ_{sc}/dT (mA cm^{-2} K^{-1}) ($\times 10^{-3}$)	$-dV_{oc}/dT$ (m V K^{-1})			$-dFF/dT$ (% K^{-1})			$-d\eta/dT$ (% K^{-1})			$-(1/\eta)(d\eta/dT)$ (% K^{-1})
		I[a]	II[a]	III[a]	I	II	III	I	II	III	III
Si	8.57	2.04	2.12	1.61	0.12	0.14	0.085	8.93	9.18	7.30	0.25
Si[a][5]	0.957		2.20			0.066			8.55		0.78
Ge	0.106	1.28	1.15	1.34	0.360	0.36	0.244	9.18	10.9	8.83	0.59
GaAs	0.196	2.30	2.39	1.88	0.0736	0.080	0.0585	6.89	7.19	5.46	0.18
InP	9.43	2.11	2.20	1.68	0.0765	0.084	0.0598	7.39	7.67	5.97	0.19
CdTe	0.121	2.04	2.13	1.61	0.0567	0.061	0.0465	5.60	5.87	4.35	0.15
CdS	6.67	2.22	2.30	1.79	0.0272	0.028	0.0244	0.93	1.02	0.55	0.04

[a] Experimental results measured on a crystalline Si solar cell in our previous work [5].
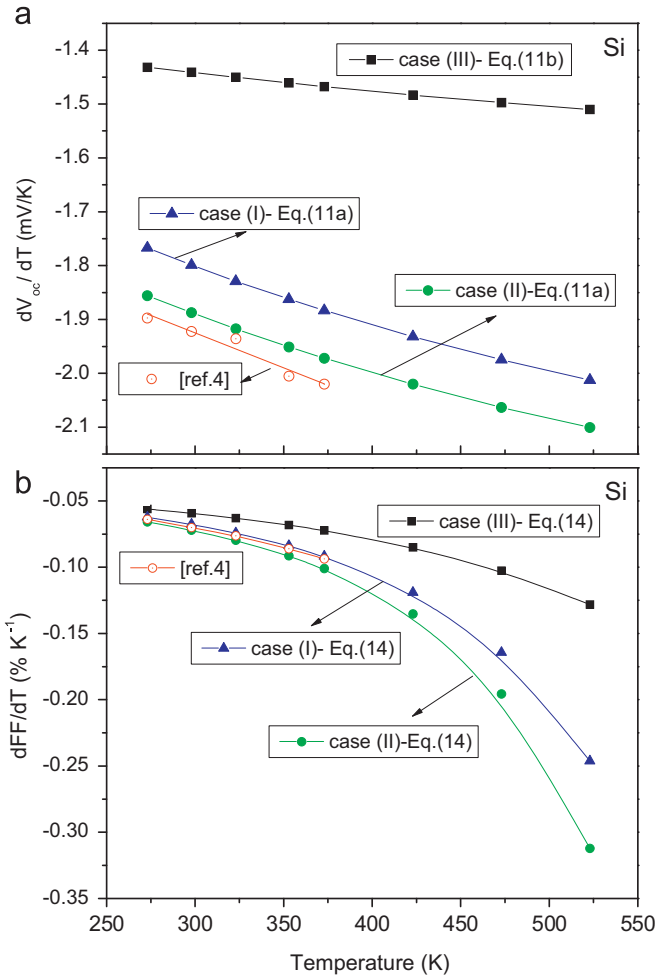
Fig. 5. Rate of change of V_{oc} and FF for Si solar cells (a) dV_{oc}/dT calculated from Eq. (10a) (cases-I and II) and (10b) (case-III). (b) dFF/dT calculated from Eq. (14) (cases-I, II and III) in the temperature range 273–523 K along with the values obtained by Fan [4].

Fig. 6. (a) Maximum achievable efficiencies for a single p–n junction solar cell at 298 K as a function of the bandgap energy for the spectra AM0, AM1.5G and AM1.5D. (b) The efficiency of solar cells as a function of bandgap and temperature (case-III) for AM1.5G.

of these parameters, dV_{oc}/dT, dFF/dT and $d\eta/dT$ may be higher for practical solar cells made from these semiconductors. In addition, the rate of decrease of these parameters is high in poorly performing solar cells as compared to good solar cells [5]. The values reported in this work are nearly same as reported in the literature [1–5]. Fig. 5a and b indicate that, as temperature changes, cases (I) and (II) are more suitable to describe the performance parameters of solar cells. It can also be seen from Fig. 5a and b that as temperature increases both dV_{oc}/dT and

dFF/dT decrease. Similar dV_{oc}/dT and dFF/dT behavior is also seen for solar cells made from GaAs, Ge, InP, CdTe and CdS (due to similarity, the plots are not shown). As can be seen from Table 3, the rate of decrease in efficiency with T is lower for solar cells made from CdS and CdTe. It can also be seen from Table 3 that the rate of decrease of efficiency with T decreases with increasing

bandgap. In earlier studies [2,3], it has been reported that the normalized temperature coefficient, $(1/\eta)\, d\eta/dT$ increases directly with increasing bandgap. In this work also, the calculated $(1/\eta)\, d\eta/dT$ increases with increasing bandgap (shown for case III only).

At this point, it will be worthwhile to present our experimental results measured on a crystalline silicon solar cell. Cell fabrication and related details have been published earlier in a paper by Priyanka et al. [5].The rate of change of performance parameters, i.e., dJ_{sc}/dT, dV_{oc}/dT, dFF$/dT$ and $d\eta/dT$ for a Si solar cell are listed in Table 3. It can be seen from Table 3 that the values are slightly different from the calculated values. dV_{oc}/dT is -2.2 mV/K which is lower than the calculated value for the three cases. This may be attributed to the higher $J_0 - 8.78 \times 10^{-6}$ mA cm^{-2} of Si solar cell [5]. In addition, the performance and diode parameters of this Si solar cell at 300 K are: V_{oc}–0.582 V, J_{sc}–25.30 mA cm^{-2}, FF–0.71, η–10.46%, R_{sh}–407Ω, R_s–0.059 Ω and n–1.52 [5]. The parameters, V_{oc}, J_{sc}, FF and η are considerably different from theoretical parameters calculated in this work which can be attributed to the resistive losses, higher J_o as well as to the higher n.

The performance parameters, V_{oc}, J_{sc}, FF and η, at 298 K for AM0 spectra for cells made from various materials are listed in Table 2. Furthermore, it is important to discuss the variation in maximum achievable efficiency with bandgap. Fig. 6a shows the maximum achievable efficiencies for a single p–n junction solar cell at 298 K as a function of the bandgap for the spectra AM0, AM1.5G and AM1.5D. It can be seen from Table 2 and Fig. 6a that, the calculated efficiencies are higher for AM1.5 spectra than AM0 as the incident power is higher for AM0 (1353 Wm^{-2}) than AM1.5 (1000 Wm^{-2}). The efficiency for spectra AM1.5 G is slightly higher than AM1.5D and the difference in efficiency may be attributed to incident power. Therefore, the incident power results in lower efficiencies for AM0 (as can be seen from Eq. (15)). As can be seen from Fig. 6a, the materials with the optimum bandgap are InP, GaAs and CdTe with a bandgap of 1.39 eV, 1.43 eV and 1.53 eV respectively having highest efficiencies of $\sim$29% at 298 K for AM1.5G spectra whereas it is $\sim$26% for AM0 spectra. It can be seen from Table 2 that the maximum efficiencies for solar cells made from the materials, calculated in this work, are very close to the values reported for AM0 spectra [2,3]. In Fig. 6a, the small peaks close to maximum efficiency (between 1 and 2 eV bandgap energy) correspond to the variation in AM1.5 spectral data due to atmospheric absorption [21]. Therefore, in Fig. 6a, at the maximum theoretical efficiency, an exact choice of the corresponding band gap or material can be made.

The performance of solar cells as a function of bandgap and temperature is shown in Fig. 6b for solar cells based on Ge, Si, InP, GaAs, CdTe and CdS in the temperature range 273–523 K. The efficiencies have been calculated for AM 1.5G spectrum for case (III). As temperature increases, efficiency decreases and the maximum achievable efficiency shifts towards higher bandgap materials. As can be seen in Fig. 6b, the optimum bandgap shifts from $\sim$1.35 eV at 273 K to $\sim$1.41e V at 523 K.

4. Conclusions

The temperature dependence of performance parameters, V_{oc}, J_{sc}, FF and η, of solar cells based on Ge, Si, GaAs, InP, CdTe and CdS has been investigated in the temperature range 273–523 K. The effect of J_o on these parameters is discussed for the three cases described in the paper. The maximum achievable V_{oc}, J_{sc}, FF and η of solar cells, calculated for AM1.5G and AM0, are nearly the same as in the literature. With increasing temperature, reverse saturation current increases, and therefore, V_{oc} decreases which decreases the fill factor and hence the efficiency of the solar cell. At the same time, the bandgap also decreases with increasing temperature and this results in an increase in J_{sc} which acts to

improve the efficiency of the cell. Therefore, the tendency of V_{oc} to decrease and J_{sc} to increase with increasing temperature in the solar cells results in a decrease in the efficiency with increasing temperature. The performance of cells for case (III) gives the best agreement between the calculated and available theoretical and experimental data for solar cells made from Si, Ge and GaAs whereas, for InP, CdTe and CdS based solar cells, case (I) seems to be more appropriate at 298 K.

The calculated rate of change of performance parameters for solar cells made from Ge, Si and GaAs with temperature, viz., dJ_{sc}/dT, dV_{oc}/dT, dFF$/dT$ and $d\eta/dT$ match fairly well with available data. The determined performance parameters of an experimental silicon solar cell and their rate of change with T are comparable to theoretical results. The rate of decrease, $-dV_{oc}/dT$, of a practical Si solar cell is higher than the ideal solar cells due to higher J_o. Moreover, as temperature changes, cases (I) and (II) are more suitable to describe the performance of solar cells.

References

[1] S.M. Sze, Physics of Semiconductor Devices, John Wiley & Sons, NewYork, 1981, p. 264 (Chapter 14).

[2] G. Landis, R. Rafaelle, D. Merritt, High temperature solar cell development, 19th European Photovoltaic Science and Engineering Conference, Paris, France, June 7–11, 2004.

[3] J.J. Wysocki, P. Rappaport, Effect of temperature on photovoltaic solar energy conversion, Journal of Applied Physics 31 (1960) 571–578.

[4] J.C.C. Fan, Theoretical temperature dependence of solar cell parameters, Solar Cells 17 (1986) 309–315.

[5] P. Singh, S.N. Singh, M. Lal, M. Husain, Temperature dependence of I–V characteristics and performance parameters of silicon solar cell, Solar Energy Materials and Solar Cells 92 (2008) 1611–1616.

[6] D.J. Friedman, Modeling of tandem cell temperature coefficients. in: 25th IEEE Photovoltaic Specialists Conference, Washington DC, IEEE, New York, 1996, pp. 89–92.

[7] M.A. Contreras, T. Nakada, A.O. Pudov, R. Sites, ZnO/ZnS(O,OH)/Cu(In,Ga)Se2/ Mo solar cell with 18.6% efficiency, in: Proceedings of the Third World Conference of Photovoltaic Energy Conversion, 2003, pp. 570–573.

[8] M.J. Jeng, Yu.L. Lee, L.B. Chang, Temperature dependences of ln$_x$Ga$_{1-x}$N multiple quantum well solar cells, Journal of Physics D: Applied Physics 42 (2009) 105101. (pp. 6).

[9] C.H. Henry, Limiting efficiencies of ideal single and multiple energy gap terrestrial solar cells, Journal of Applied Physics 51 (1980) 4494–4500.

[10] W. Shockley, H.J. Queisser, Detailed balance limit of efficiency of p–n junction solar cells, Journal of Applied Physics 32 (1961) 510–519.

[11] D. Vos, C.C. Grosjean, H. Pauwels, On the formula for the upper limit of photovoltaic solar energy conversion efficiency, Journal of Physics D: Applied Physics 15 (1982) 2003–2015.

[12] Luque, S. Hegedus, Handbook of Photovoltaic Science and Engineering, Wiley-Sons, 2003.

[13] N. Posthuma, J. van der Heide, G. Flamand, J. Poortmans, Emitter formation and contact realization by diffusion for germanium photovoltaic devices, IEEE Transactions on Electronic Devices 54 (5) (2007) 1210–1215.

[14] Riordan, R. Hulstron, What is an air mass 1.5 spectrum?, in: Proceedings of the Conference Record 21st IEEE Photovoltaic Specialists Conference 2, 1990, pp. 1085–1124.

[15] American Society for Testing and Materials (ASTM). Reference solar spectral irradiance: Air mass 1.5. Available: ⟨http://rredc.nrel.gov/solar/spectra/am1.5/⟩.

[16] M.P. Thekaekara, Extraterrestrial solar spectrum, 3000–6100 A at 1-A intervals, Applied Optics 13 (1974) 518–522.

[17] Y.P. Varshni, Temperature dependence of the energy gap in semiconductors, Physica 34 (1967) 149–154.

[18] N.M. Ravindra, V.K. Srivastava, Temperature dependence of the energy gap in semiconductors, Journal of Physics and Chemistry of Solids 40 (1979) 791–793.

[19] R. Pässler, Parameter sets due to fittings of the temperature dependencies of fundamental bandgaps in semiconductors, Physica Status Solidi (b) 216 (1999) 975–1007.

[20] C. Hu, R.M. White, Solar Cells, McGraw-Hill, New York, 1983, pp. 21.

[21] M.E. Nell, A.M. Barnett, The spectral p–n junction model for tandem solar-cell design, IEEE Transactions on Electron Devices 24 (1987) 257–266.

[22] M.A. Green, Solar Cells, Prentice-Hall, Englewood Cliffs, NJ, 1982, p. 88.

[23] J.J. Loferski, Theoretical considerations governing the choice of the optimum semiconductor for photovoltaic solar energy conversion, Journal of Applied Physics 27 (1956) 777–784.

[24] J.C.C. Fan, B.Y. Tsaur, B.J. Palm, Optimal design of high efficiency tandem cells, in Conference Record 16th IEEE Photovoltaic Specialists Conference, 1982, pp. 692–701.

[25] A. Rockett, The Materials Science of Semiconductors, Springer, 2008, pp. 84.

[26] T. Markvart, L. Castaner (Eds.), Elsevier, Oxford, 2005., pp. 58–67 452–503:/ ⟨http://www.sciencedirect.com/science/book/9781856174572S⟩, accessed on 12/14/2007.

[27] Editorial, Reporting solar cell efficiencies in solar energy materials and solar cells, Solar Energy Materials and Solar Cells 92 (2008) 371–373.

[28] M.A. Green, Keith Emery, Yoshihiro Hishikawa, Wilhelm Warta, Solar cell efficiency tables (version 37), Progress in Photovoltaics: Research and Applications 19 (2011) 84–92.

[29] G. Landis, Review of Solar Cell Temperature Coefficients for Space, Proceedings of the XIII Space Photovoltaic Research and Technology Conference, NASA CP-3278, NASA Lewis Research Center, June 1994, pp. 385–400.

[30] First Solar, First solar sets world record for CdTe solar PV efficiency, 2011, ⟨http://investor.firstsolar.com/releasedetail.cfm?ReleaseID=593994⟩.